Control of chaos by oscillating feedback

H. G. Schuster* and M. B. Stemmler
Computation and Neural Systems Program, California Institute of Technology 139-74, Pasadena, California 91125
(Received 16 August 1996; revised manuscript received 31 March 1997)

Parametric feedback control of chaos relies on detailed knowledge of the locations of unstable periodic orbits. We show that unstable periodic orbits of dynamical systems with unknown locations but known periodicity τ can be stabilized by an oscillating feedback term proportional to ε^t $(\vec{x}^t-\vec{x}^{t-\tau})$, where $\vec{x}^t$ is the location of the trajectory at time t and ε^t is periodic in time. Periodic feedback overcomes the limitations of Giona's theorem [Nonlinearity **4**, 911 (1991)], which states that constant feedback (i.e., a time-independent ε) can stabilize an unstable periodic orbit *only* if the stability matrix has no positive eigenvalues greater than unity. As an application of oscillating feedback, we use it to stabilize the memory patterns in an associative memory (Hopfield [Proc. Natl. Acad. Sci. USA **79**, 2554 (1982); **81**, 3088 (1984)]) network, thereby enhancing the total capacity of the memory device. We extend our method to high-dimensional systems described by differential equations; in this framework, it is possible to stabilize the spatiotemporal chaos generated by the Kuramoto-Sivashinsky equation [G. J. Sivashinsky and D. M. Michelson, Prog. Theor. Phys. **63**, 2122 (1980)]. [S1063-651X(97)10911-4]

PACS number(s): 05.45.+b, 47.20.−k

I. INTRODUCTION

Many nonlinear dynamical systems display chaos [1]. Recently, a general approach [2] to controlling chaos in physical systems has been proposed that is based on the existence of unstable periodic orbits within the strange attractor. The original technique, due to Ott, Grebogi, and Yorke (OGY), relies on the local linearization of the Poincaré map near an unstable periodic orbit [2]. Once the local map is known, one can apply linear feedback control to stabilize the orbit. In principle, the method of OGY is applicable to any physical system as long as the iterates of the Poincaré map can be obtained [3]. Recently, Hunt [4] has demonstrated experimentally that changing the control parameter of the chaotic system in proportion to the difference between the desired orbit and the actual trajectory is sufficient to achieve robust control. This form of parametric feedback control has been applied to several experimental systems [5] and underpinned theoretically [6]. However, in order to apply Hunt's method, it is necessary to know the location of the orbit that one wants to stabilize or, if this is not the case, one could choose an arbitrary point on the attractor and stabilize the least-unstable periodic orbit in its vicinity. In this article, we will present a method for chaos control that is as simple as Hunt's method but does not require knowledge of the orbit's location. Instead, the method will stabilize orbits of a prescribed periodicity. This approach is of some theoretical and practical importance for the following reasons.

(i) The set of unstable periodic orbits is dense in the Poincaré map of a chaotic dynamical system. The locations of these orbits, starting with unstable cycles of period 2, trace out the skeleton of the chaotic attractor. The control method described here allows one to find experimentally all unstable periodic orbits of a given periodicity without any prior knowledge of the chaotic system.

(ii) The method generalizes easily to higher-dimensional systems and can be applied to dynamical systems that are not intrinsically chaotic but possess unstable fixed points into which one wants to trap the system. One example of a non-chaotic system with unstable fixed points is the Hopfield model [7] of associative memory, in which the fixed points of the dynamical system correspond to stored memory patterns. If the number of memory patterns is small, the trajectory of the system will move from an arbitrary input pattern to the closest fixed point, which is the best match to a ''memory.'' Attempts to store too many memory patterns are thwarted by the fixed points (or memory patterns) becoming unstable. Our method stabilizes the fixed point closest to the current trajectory, thereby increasing the number of patterns that can be stored and retrieved.

(iii) Our method, which will first be introduced for dynamical systems described by maps, can be extended to systems described by differential equations. We will demonstrate that the spatiotemporal chaos generated by the Kuramoto-Sivashinsky equation [8], which describes the fluctuations in the height of a fluid film moving on an inclined plane under the influence of gravity, can be ''tamed'' by periodic feedback.

As we will see in the following sections, our method consists of applying delayed feedback control to the system. In the context of chaos control, delayed feedback was originally proposed by Pyragas [9] and has been applied to control chaos in neodymium-doped lasers [10]. The different point of our method is to overcome an important limitation that occurs for delayed feedback control. As proved rigorously by Giona [11], delayed feedback control will only work (for systems described by Poincaré maps) if the local stability matrix of the unstable periodic orbit that one wants to stabilize has only negative unstable eigenvalues. Similar restrictions hold for systems described by differential equations. It will be shown that these restrictions can be overcome by modulating the feedback control periodically.

*Permanent address: Institut für Theoretische Physik, Universität Kiel, Olshausenstrasse 40, D-24098 Kiel, Germany.

In the following, we will first show how our method stabilizes unstable fixed points in one-dimensional maps (Sec. II). Then we will apply the method to the Hopfield model (Sec. III and the Appendix). In Sec. IV, we will introduce periodic feedback for higher-dimensional systems described by differential equations and demonstrate the application of periodically modulated, delayed feedback control to the Kuramoto-Sivashinsky equation of fluid dynamics. We conclude with a brief discussion in Sec. V.

II. STABILIZATION OF UNSTABLE FIXED POINTS IN SYSTEMS DESCRIBED BY MAPS

We start from a one-dimensional map

$$x^{t+1}=f(x^t), \tag{2.1}$$

where t is the discrete time, and linearize it in the vicinity of an unstable fixed point $x^*=f(x^*)$. This leads to

$$x^{t+1}=\lambda x^t, \tag{2.2}$$

where $\lambda=(d/dx)f(x^*)$ such that $|\lambda|>1$. We can assume without restricting our arguments that $x^*=0$. In order to stabilize the fixed point, we add a perturbation $\varepsilon(x^t-x^{t-1})$ to the map of Eq. (2.1), which represents a delayed feedback term that does not change the location of the fixed point but influences its stability, as has been observed by Pyragas [9]. This modifies Eq. (2.1) to

$$x^{t+1}=f[x^t+\varepsilon(x^t-x^{t-1})]. \tag{2.3}$$

Linearization around $x^*=0$ leads to

$$x^{t+1}=\lambda x^t+\varepsilon\lambda(x^t-x^{t-1}). \tag{2.4}$$

Giona [11] proved that the addition of delay terms of arbitrary order to a map can only stabilize the fixed point only if $\lambda<0$. An intuitive picture of why this is so can be drawn as follows: If the sign of x^t alternates on successive iterates because $\lambda<0$, then the stabilizing term $\varepsilon(x^t-x^{t-1})$ vanishes less rapidly and hence has more effect on the stability of x^*, than for $\lambda>0$, in which case both x^t and x^{t-1} converge with the same sign to x^*. If we make the ansatz $x\sim\gamma^t$ in Eq. (2.4), we obtain $\gamma_\pm=\frac{1}{2}\{\lambda(1+\varepsilon)\pm\sqrt{[\lambda(1+\varepsilon)]^2-4\varepsilon\lambda}\}$. The requirement that $|\gamma|<1$ leads to the stability region delineated by the solid lines in Fig. 1. The stability region is confined to $\lambda<1$, in agreement with Giona's theorem. [The delay term stabilizes the fixed point for $\lambda\leqslant-1$; for $-1<\lambda<1$ the fixed point in Eq. (2.4) is already stable for $\varepsilon=0$.]

If we want to stabilize also fixed points with $\lambda>1$, we must avoid a too rapid decay of the difference $\varepsilon(x^t-x^{t-1})$. This could be achieved by making ε time dependent. The simplest choice $\varepsilon^t=0$ for t odd and $\varepsilon^t=\varepsilon\neq0$ for t even will allow stabilization of both positive and negative λ [12]. With this, Eq. (2.4) becomes

$$x^{t+1}=\lambda x^t, \tag{2.5a}$$

$$x^{t+2}=\lambda x^{t+1}+\lambda\varepsilon(x^{t+1}-x^t), \tag{2.5b}$$

which can be rewritten as

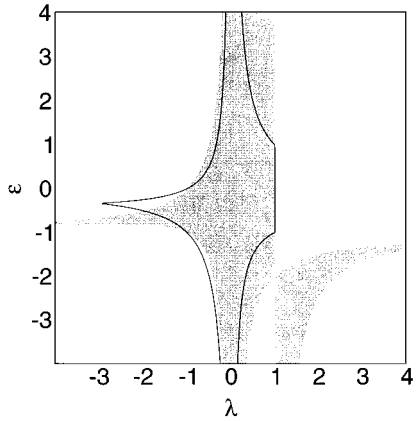

FIG. 1. Stability region in the ε,λ plane for periodic (shaded area) and nonperiodic (area delineated by the solid lines) feedback control.

$$x^{t+1}=\lambda x^t, \tag{2.6a}$$

$$x^{t+2}=\lambda[\lambda+\varepsilon(\lambda-1)]x^t. \tag{2.6b}$$

As shown in Fig. 2, x^t jumps between two linear maps with different slopes. The slope of the lower branch could, by an appropriate choice of ε, always be made small enough to ensure the stability of $x^*=0$. This means formally that the effective slope $\lambda[\lambda+\varepsilon(\lambda-1)]$in the map $x^{t+2}=\gamma x^t$ could always be made smaller than unity. The condition for stability $|\gamma|<1$ yields for the boundaries $\gamma_\pm=\pm1$

$$\varepsilon_+=-(1+\lambda)/\lambda,\quad \varepsilon_-=-(1+\lambda^2)/[\lambda(\lambda-1)]. \tag{2.7}$$

The stability region $|\gamma|<1$ is shown as the shaded area (with boundaries $\varepsilon_\pm$) in Fig. 1. With oscillatory delayed feedback, the stability region extends into the region of positive $\lambda>1$. A single value of ε can stabilize a range of unstable eigenvalues, which will become important for high-dimensional sytems where we want to stabilize a whole spectrum of unstable λ values by a single control parameter [13].

To stabilize higher-order unstable fixed points, one can add to the map $x^{t+1}=\lambda x^t$ a delayed feedback term $\varepsilon^t(x^t-x^{t-\tau})$, where $\varepsilon^t=0$ for $0\leqslant t<\tau$ and $\varepsilon^t=\varepsilon$ for $t=\tau$. In analogy to Eq. (2.6), we obtain $x^{t+\tau+1}=\gamma x^t$ with $\gamma=\lambda^\tau[\lambda+\varepsilon(\lambda-1)]$. A cycle of period τ is stable if $|\gamma|<1$. Stabili-

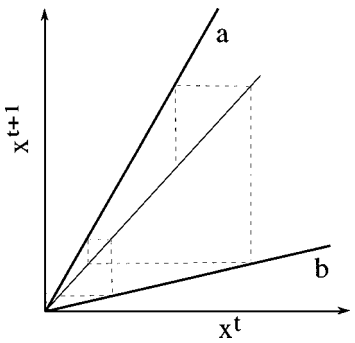

FIG. 2. For periodic feedback control the trajectory (dotted line) approaches the fixed point by jumping between two linear maps (a) $x^{t+1}=\lambda x^t$ and (b) $x^{t+2}=(\lambda+\lambda\varepsilon-\varepsilon)x^{t+1}$.

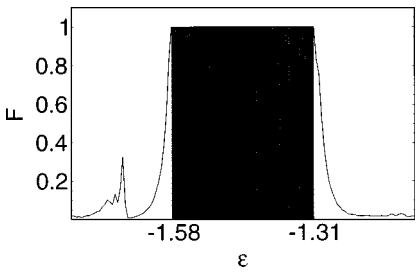

FIG. 3. Oscillatory delayed feedback control of the twofold iterated logistic map $f^2(x)=r^2x^2(1-x)^2$ for $r=3.8$. Displayed in the graph is the fraction F of iterates that remain after a random injection of an initial point into the interval $I=x^*\pm10^{-2}$ around the fixed point $x^*=1-(1/r)$ after ten iterations of the map f^2. The slope of the map f^2 at the fixed point $x^*=0.737$ is $\lambda=3.24$; since the slope is greater than unity, the map cannot be controlled by constant delayed feedback. Within the shaded area, in agreement with Eq. (2.7), the map controlled by oscillatory delayed feedback is absolutely stable.

zation can always be achieved with an appropriate choice of ε, as for simple fixed points, which have the periodicity $\tau=1$.

As a straightforward application of the method, we use periodic feedback to stabilize the unstable fixed point of the twofold iterated logistic map, which could not be stabilized by constant delay terms because of Giona's theorem. Figure 3 shows the fraction of iterates that, after the starting point x^0 had been injected randomly into the interval $I=x^*\pm10^{-2}$, remained within I. There exists a finite range of ε values that stabilize the fixed point completely. For unmodulated feedback the fraction of iterates that remain in the interval I is below 1

III. STABILIZATION OF PATTERNS IN THE HOPFIELD MODEL

The symmetric Hopfield model [7] is a variation on the Ising model for simple magents with $i=1,\ldots,N$ graded spins S_i connected by an interaction matrix $J_{ij}=(1/N)\Sigma_\mu\xi_i^\mu\xi_j^\mu$. The matrix J_{ij} stores $\mu=1,\ldots,p$ random patterns $\xi_i^\mu=\pm1$ and is by construction symmetric $J_{ij}=J_{ji}$. The patterns $\vec{\xi}^\mu$ are known as memory patterns.

Starting from an arbitrary initial pattern $\vec{S}^0$ (with $-1\leqslant S_i^0\leqslant1$), the Hopfield model evolves according to the dynamical rules [14]

$$S_i^{t+1}=\tanh[\beta h_i^t], \tag{3.1}$$

where

$$h_i^t=\frac{1}{N}\sum_{j=1}^{N}J_{ij}S_j^t \tag{3.2}$$

is the local ''magnetic'' field for the ith spin, generated by all other spins through the interaction matrix J_{ij}. At each time step of the dynamics, the spin S_i^t will tend to align itself parallel to the local field. In fact, in the limit of $\beta\to\infty$, Eq. (3.1) becomes

$$S_i^{t+1}=\mathrm{sgn}[h_i^t] \tag{3.3}$$

and the alignment of S_i^{t+1} to the local field becomes perfect. Only a nonzero temperature, entering through the factor $\beta=(1/T)$ in Eq. (3.1), will counteract the tendency of spins to align perfectly.

The crucial feature of the symmetric Hopfield model is that it admits a Lyapunov function, or generalized energy function, that governs the dynamics [7]. Continuing the analogy to a magnet, the alignment of spins parallel to their local field lowers the total energy of the Hopfield model

$$L^t=-\sum_{i,j=1}^{N}J_{ij}S_i^tS_j^t \tag{3.4}$$

with each time step, such that $L^{t+1}\leqslant L^t$. In the long-time limit, the system moves to a stable state with minimal energy. If the initial state of the spins $\vec{S}^0$ is close to one of the stored patterns, say $\vec{\xi}^1$, then the system state will move towards the stored pattern. To illustrate, we consider the simplest case, where $\vec{\xi}^1$ is the only pattern stored in the network and thus $J_{ij}=(1/N)\xi_i^1\xi_j^1$. In the zero-temperature limit

$$\begin{aligned}L^t&=-\sum_{i,j=1}^{N}J_{ij}S_i^tS_j^t\\&=-\frac{1}{N}\sum_{i,j=1}^{N}\xi_i^1\xi_j^1S_i^tS_j^t=-\frac{1}{N}\left[\sum_{i=1}^{N}\xi_i^1S_i^t\right]^2=-\frac{1}{N}(\vec{\xi}^1\cdot\vec{S}^t)^2\end{aligned} \tag{3.5}$$

and we can see directly that the minimal energy is achieved if the vector $\vec{S}^t=(S_1^t,\ldots,S_N^t)$ points parallel (or antiparallel) to the pattern $\vec{\xi}^1$. In other words, the minimum-energy configuration $\lim_{t\to\infty}L^t$ corresponds to a stored pattern or memory of the network. Lyapunov functions also exist for Hopfield models at nonzero temperatures.

Generalizing Eq. (2.3) to N dimensions, we introduce delayed feedback into the Hopfield model as

$$S_i^{t+1}=\tanh\left[\beta\sum_{j=1}^{N}J_{ij}S_j^t\right], \tag{3.6a}$$

$$S_i^{t+2}=\tanh\left[\beta\sum_{j=1}^{N}J_{ij}[(1+\varepsilon)S_j^{t+1}-\varepsilon S_j^t]\right], \tag{3.6b}$$

where β is the inverse temperature. As in Eq. (2.5), the delayed feedback term has been made oscillatory.

In the original Hopfield model, the fact that $L^{t+1}<L^t$ implies that only simple fixed points are allowed to exist. With delayed feedback, stable two-cycles become possible in the Hopfield model [15], in addition to the usual stable fixed points. To show that the oscillating delay term can stabilize two-cycles, we construct a Lyapunov function L for two-cycles, following the seminal work of Amit [16]:

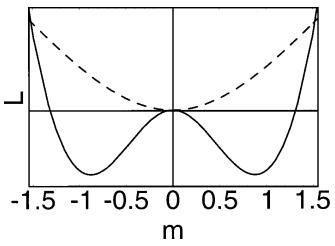

FIG. 4. Lyapunov function $L(m)$ of the Hopfield model with one stored pattern. The dotted lines correspond to $L(m)$ without feedback for $\beta=0.5$. The full lines correspond to $L(m)$ for the same values of β after periodic feedback with $\varepsilon=-5$ has been switched on.

$$L=\sum_{i,j} J_{ij}S_i^t\left[(1+\varepsilon)S_j^{t+1}-\frac{\varepsilon}{2}S_j^t\right]$$
$$-\frac{1}{\beta}(1+\varepsilon)\sum_i \ln\left[\cosh\left(\beta\sum_j J_{ij}S_j^t\right)\right]$$
$$-\frac{1}{\beta}\sum_i \ln\left[\cosh\left(\beta\sum_j J_{ij}[(1+\varepsilon)S_j^{t+1}-\varepsilon S_j^t]\right)\right]. \quad (3.7)$$

To get acquainted with the influence of the delay terms, we first investigate the Hopfield model with only one stored pattern $\vec{\xi}^1$. By introducing the overlap $m^t=(1/N)\Sigma_i\xi_i^1S_i^t$ between the state vector $\vec{S}^t$ and the pattern $\vec{\xi}^1$, the equations of motion reduce to

$$m^{t+1}=\tanh(\beta m^t), \quad (3.8a)$$

$$m^{t+2}=\tanh\{\beta[(1+\varepsilon)m^{t+1}-\varepsilon m^t]\} \quad (3.8b)$$

and the Lyapunov function L becomes

$$L=(1+\varepsilon)m\tanh(\beta m)-\frac{\varepsilon}{2}m^2-\frac{(1+\varepsilon)}{\beta}$$
$$\times\ln[2\cosh(\beta m)]-\frac{1}{\beta}\ln(2\cosh$$
$$\times\{\beta[(1+\varepsilon)\tanh(\beta m)-\varepsilon m]\}). \quad (3.9)$$

Figure 4 shows L for different values of β and ε. We note that for high temperatures ($\beta\to 0$) the choice of a large enough (negative) ε will always stabilize a two-cycle: For $\beta\ll 1$, Eq. (3.8a) yields $m^{t+1}=\beta m^t$ and Eq. (3.8b) becomes $m^{t+2}=\tanh\{\beta[\beta(1+\varepsilon)-\varepsilon]m^t\}\cong\tanh[\beta(-\varepsilon)m^t]$ for $-\varepsilon\gg 1$. This means that large (negative) ε values lead to an effective $\beta_{eff}=\beta(-\varepsilon)$ that compensates for the small value of the original β.

The use of the Hopfield model as an associative memory is limited by the number of patterns $\vec{\xi}^\mu$ that can be stored and retrieved relative to the total number of spins. The ratio $\alpha=p/N$ is commonly known as the capacity, where p is the number of memory patterns and N the number of spins. At zero temperature ($\beta\to\infty$), the original Hopfield model has a capacity of $\alpha=0.138$ in the limit as $N\to\infty$. Storing a number of patterns greater than $p=\alpha N$ has catastrophic effects: The memory patterns become unstable fixed points, rendering the associative memory device useless. In this case, the Hopfield model evolves towards an unintelligible superposition of memory patterns (a spin-glass state) or to a paramagnetic state which has, on average, no overlap with any stored pattern $\vec{\xi}^\mu$.

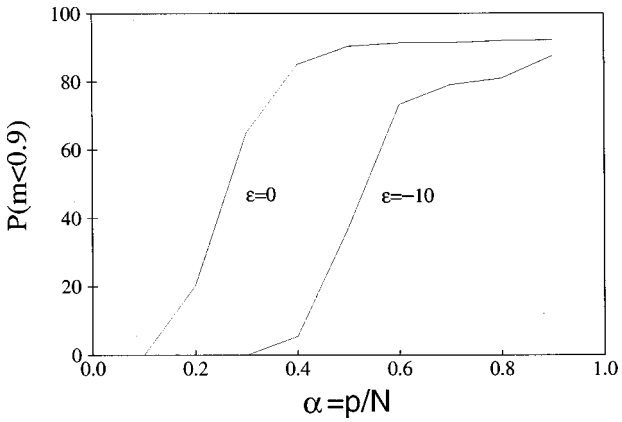

FIG. 5. Enhancement of the capacity of the Hopfield model due to periodic feedback for high temperatures. We start from a perfectly aligned pattern, i.e., $m=1$. After 500 runs with different initial patterns we show the probability $P(m<0.9)$ in percent that in the long-time limit m becomes smaller than $m=0.9$, as a function of α, for $\beta=0.2$ and $\varepsilon=-10$ as compared to $\varepsilon=0$ and $\beta=2$ [18].

Since delayed feedback stabilizes unstable fixed points, one might expect that such feedback could increase the capacity of the Hopfield model. The net effect of constant, nonoscillatory delay terms in the Hopfield model is to weakly stabilize stored patterns [17]. But how does oscillating delayed feedback change the capacity of the Hopfield model?

For $\beta\to 0$ and more than one memory pattern, we can stabilize a two-cycle that describes the time dependence of $m^t=(1/N)\Sigma_i\xi_i^\mu S_i^t$, i.e., the projection of the pattern vector $\vec{S}^t$ onto a stored pattern $\vec{\xi}^\mu$. Since the memory patterns are chosen randomly, the results are independent of the choice of ξ^μ. Figure 5 shows that the oscillating term not only raises β to the effective value $\beta|\varepsilon|$, as in the case of only one stored pattern considered above, but also has a stabilizing effect on the patterns such that the capacity increases up to $\alpha=0.6$.

For $\beta\to\infty$, oscillating feedback leads again to a stabilization of the patterns but this time the effect is most pronounced for $\varepsilon=-2$ (see Fig. 6). We can understand this from Fig. 1, where we see that $\varepsilon=-2$ stabilizes all eigenvalues λ in the range $1-\sqrt{2}<\lambda<1+\sqrt{2}$. This means that if the stability matrix of a stored pattern $(\partial S_i^{t+2}/\partial S_j^t)[\vec{\xi}^\mu]$ that can be computed directly from Eqs. (3.6) and is (because the derivative is taken at $\vec{\xi}^\mu$) independent of t contains eigenvalues larger than 1 such that the pattern becomes unstable, then the delay term with $\varepsilon=-2$ makes these eigenvalues smaller than one such that the pattern becomes stable. In the Appendix we present an analytical computation of the capacity of the Hopfield model as a function of ε. It shows that not only ''fast noise generated by a finite temperature'' but also ''self generated noise that stems from the uncondensed patterns'' [15] becomes suppressed by an oscillating delay term. The effect is strong enough to enhance the capacity of the Hopfield model by an order of magnitude.

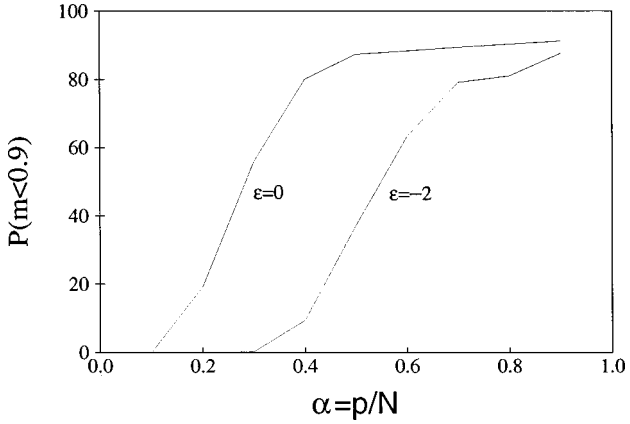

FIG. 6. Enhancement of the capacity of the Hopfield model due to periodic feedback for low temperatures. We start from a perfectly aligned pattern ($m=1$). After 500 runs we show the probability $P(m<0.9)$ in percent that in the long-time limit m becomes smaller than $m=0.9$, as a function of α, for $\beta=20$ and $\varepsilon=0$ as compared to $\beta=20$ and $\varepsilon=-2$.

In principle, oscillating delay terms could be realized biologically. We envision the delayed feedback to be carried by inhibitory association fibers [18]. In the canonical microcircuit model of cortex [19], for instance, these inhibitory synapses are themselves subject to shunting inhibition. The character of the feedback will be oscillatory if the inhibition of these inhibitory synapses is periodic.

IV. STABILIZATION OF CHAOTIC SYSTEMS THAT ARE DESCRIBED BY DIFFERENTIAL EQUATIONS

In this section we extend our results for maps to differential equations. In order to keep things simple we first demonstrate how one could stabilize an unstable fixed point of a single differential equation. It is understood that one ordinary differential equation cannot generate chaos [1], but our results could then be transferred in a straightforward fashion to sets of three or more differential equations that are capable of producing chaotic behavior. Let us first try to stabilize the unstable ($\mathrm{Re}\lambda>0$) fixed point of

$$\dot{x}=\lambda x \tag{4.1}$$

at the origin by adding a delay term

$$\dot{x}=\lambda x+\varepsilon[x(t)-x(t-\tau)], \tag{4.2}$$

with time-independent $\varepsilon$and delay time τ. With the ansatz $x\sim\exp(\gamma t)$ we find $\gamma=\lambda+\varepsilon[1-\exp(-\gamma\tau)]$. Figure 7 shows the regions in complex λ space for which $\mathrm{Re}\gamma<0$, i.e., for which delay with constant ε stabilizes the fixed point. It follows that for $\mathrm{Im}\lambda=0$ the unstable fixed point could not be stabilized at all. Only for $\mathrm{Im}\lambda\neq 0$, i.e., only if originally the trajectory escaped from the fixed point in an oscillatory fashion, can we stabilize it in a, relatively small, λ region. This corresponds to Giona's observation for discrete systems where one could stabilize a fixed point with a constant delay term only if the original trajectory displayed oscillations due to the negative sign of the local slope. It is shown in Ref.

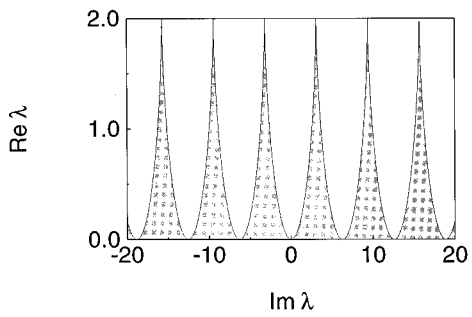

FIG. 7. Stability region of Eq. (4.1) for $\tau=1$ and $\varepsilon=-2$ in the complex λ plane. The region terminates at $\mathrm{Re}\lambda=-\varepsilon$ and is periodic in $\mathrm{Im}\lambda$. Note that the whole $\mathrm{Re}\lambda$ axis is unstable.

[20] that simply making ε oscillating in Eq. (4.2) will not help. Instead we have to add an oscillating velocity term such that Eq. (4.1) becomes

$$\dot{x}=\lambda x+\varepsilon^t\dot{x}(t-\tau). \tag{4.3}$$

In Eq. (4.3) ε^t changes periodically between zero and a constant value: $\varepsilon^t=0$ for $n\tau\leqslant t<(n+1)\tau$ and $\varepsilon^t=\varepsilon\neq 0$ for $(n+1)\tau\leqslant t<(n+2)\tau$, where $n=0,2,4,\ldots$.

In order see that the the fixed point in Eq. (4.3) could indeed be stabilized by an appropriate choice of ε, we integrate Eq. (4.3) over two intervals of τ. For $n\tau\leqslant t<(n+1)\tau$ we obtain

$$x(t)=x(n\tau)e^{\lambda(t-n\tau)}. \tag{4.4}$$

In order integrate Eq. (4.3) in the regime $(n+1)\tau\leqslant t<(n+2)\tau$, we need to know the delay term $\dot{x}(t-\tau)$ only in the previous time interval where ε was zero. This yields

$$x[(n+2)\tau]=e^{\lambda\tau}(e^{\lambda\tau}+\lambda\varepsilon)x[n\tau]. \tag{4.5}$$

In this way we reduced the solution of Eq. (4.3) to a map that converges to the origin if $|e^{\lambda\tau}(e^{\lambda\tau}+\lambda\varepsilon)|<1$. Note that this requirement could always be met by a finite ε value. We shall see below that, as for maps, a single ε value stabilizes a whole range of unstable λ values.

As an example, we tame the spatiotemporal chaos of the Kuramoto-Sivashinsky equation [8] with our method. Chaos control in this context has been previously investigated by Petrov, Mihaliuk, Scott, and Showalter [21] without using oscillating delayed feedback. The Kuramoto-Sivashinsky equation is given by

$$\varphi_t+\varphi\varphi_x+\varphi_{xx}+\varphi_{xxxx}=0 \tag{4.6}$$

and describes the fluctuations in the (scaled) height $\varphi(x,t)$ of a thin fluid film that moves on an inclined plane under the influence of gravity. The indices in Eq. (4.6) denote partial derivatives with respect to time t and one-dimensional space x.

We choose periodic boundary conditions over a length L. Linear stability analysis of the homogeneous state $\varphi=0$ yields, with the ansatz $\varphi(x,t)\sim\exp(-\lambda t+kx)$, the stability condition $\lambda=k^4-k^2>0$. The spatially homogeneous state is unstable for all Fourier modes with wave vectors $|k|<1$. In order to stabilize the homogeneous state we have to make all

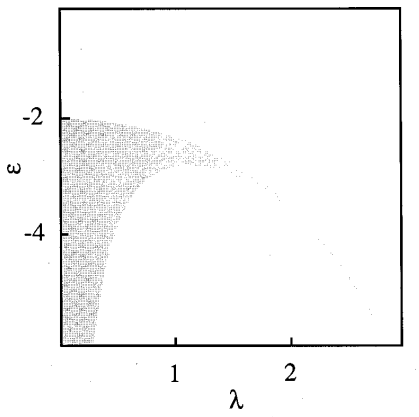

FIG. 8. Stability region of Eq. (4.3) in the ε-λ plane.

eigenvalues λ within the interval $0<\lambda<0.25$. smaller than zero. Note that the eigenvalues are all real, i.e., according to Fig. 7 a constant value of ε will not work at all. By adding to Eq. (4.6) a periodic feedback term [as in Eq. (4.3], we obtain

$$\varphi_t+\varphi\varphi_x+\varphi_{xx}+\varphi_{xxxx}+\varepsilon^t\varphi_t^{t-\tau}=0. \tag{4.7}$$

Figure 8 shows the stability region of Eq. (4.7). The homogeneous state can be stabilized, for instance, by choosing $\varepsilon=-3$, as shown in Fig. 9.

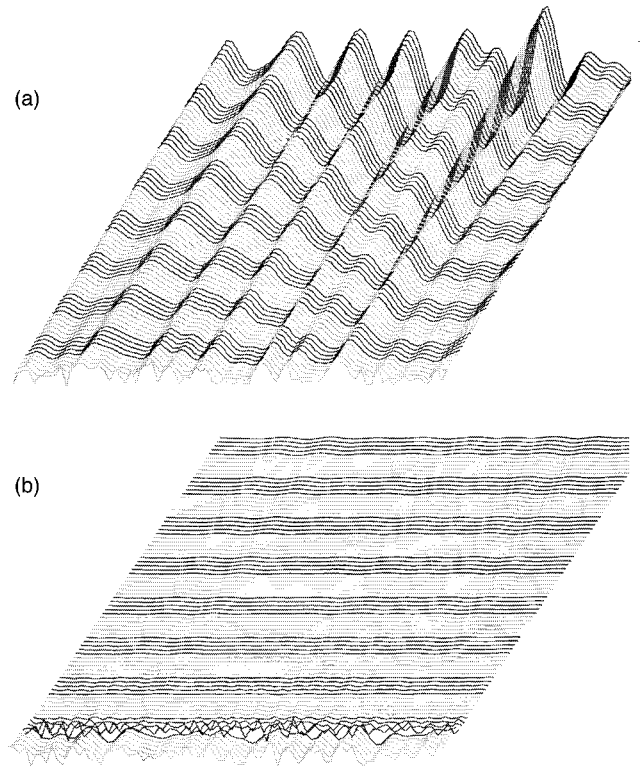

FIG. 9. Solution of the Kuramoto-Sivashinsky equation (4.6) as a function of space (horizontal axis) and time starting from random $\varphi(x,0)$ and periodic boundary conditions over an interval $L=80$. (a) Without feedback control the spatially homogeneous state is unstable. (b) For periodic feedback with $\varepsilon=-3$ and $\tau=5\,\delta t$ discretization steps, $\delta t=0.1$, the homogeneous state becomes stabilized. The shading indicates the time intervals, of size τ, where the feedback is switched on (gray) and off (black).

V. SUMMARY

We have shown that fixed points of dynamical systems described by high-dimensional maps or sets of differential equations can be stabilized by periodic delayed feedback. In the following, we briefly discuss the the influence of noise.

If we add to the map $x^{t+1}=\lambda x^t+\varepsilon^t(x^t-x^{t-1})$ a Gaussian noise term η^t with $\langle\eta^t\eta^t\rangle=\sigma^2$, we obtain from the equation of motion $x^{t+1}=\lambda x^t+\varepsilon^t(x^t-x^{t-1})+\eta^t$ directly $\lim_{t\to\infty}\langle(x^t)^2\rangle=s\sigma^2/(1-\Gamma^2)$ where $\Gamma^2=\lambda(\lambda+\varepsilon-\varepsilon/\lambda)$ and $s=1+(\lambda+\varepsilon)^2$. If we compare this to the situation with $\varepsilon=0$, i.e., $\lim_{t\to\infty}\langle(x^t)^2\rangle=\sigma^2/(1-\lambda^2)$, we see that the mean squared fluctuations around the stabilized fixed point ($\varepsilon\neq0$) are enhanced by a factor $s=1+(\lambda+\varepsilon)^2$. This is the price we must pay for stabilization.

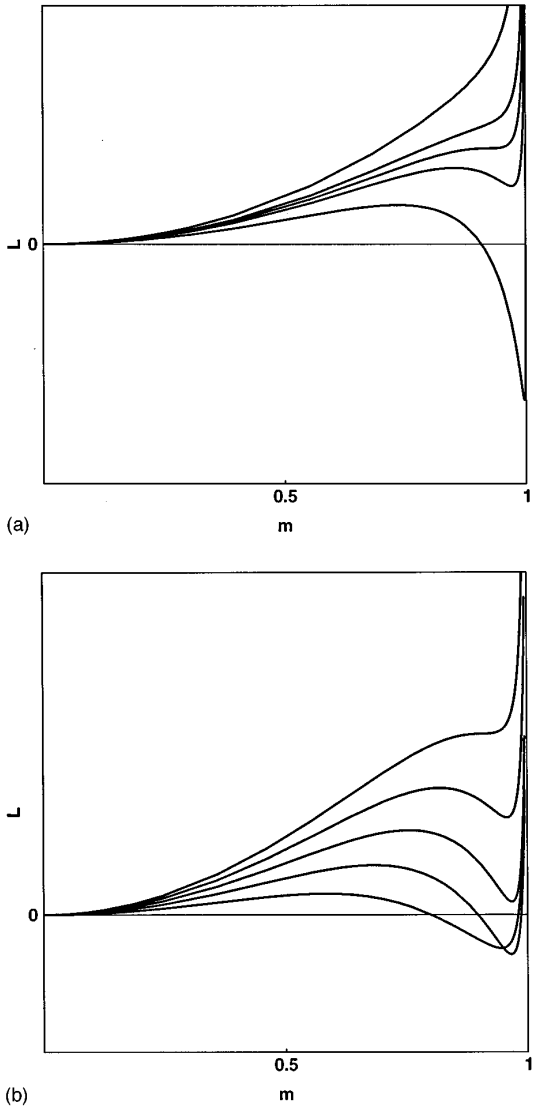

FIG. 10. Lyapunov function $L(m)$ of the Hopfield model as a function of the overlap with a stored pattern m for different values of α. (a) Without feedback: α varies as $\alpha=0.05,0.1,0.12,0.14,0.2$ between the bottom and the top curve. Note that the minimum of $L(m)$ vanishes for $\alpha=0.14$. (b) With periodic feedback and $\varepsilon=-2$: α varies as $\alpha=0.2,0.4,0.6,0.8,1$ between the bottom and the top curve. Note that the minimum in $L(m)$ now persist up to $\alpha=1$, but its stability (depths) is reduced as compared to the unstabilized situation with $\varepsilon=0$ and $\alpha=0.05$, say.

In conclusion, periodic delayed feedback overcomes the limitations of Giona's theorem and offers the possibility to stabilize spatiotemporal patterns, opening the door to many applications. One could speculate that the stabilizing combination of delay and oscillations, found above, might be one of the reasons why both elements are so often present in biological systems [22].

ACKNOWLEDGMENTS

H.G.S. thanks C. Koch for the kind hospitality extended to him at Caltech and the Deutsche Forschungsgemeinschaft for financial support. M.B.S. is funded by the Howard Hughes Medical Institute.

APPENDIX: THE CAPACITY OF THE STABILIZED HOPFIELD MODEL

The dynamical equations (3.6) yield in the infinite-time limit the two-cycle

$$\overline{S_i}=\tanh\left[\frac{\beta}{N}\sum_{\mu,j}\ \xi_i^\mu\xi_j^\mu S_j\right], \tag{A1}$$

$$S_i=\tanh\left[\frac{\beta}{N}\sum_{\mu,j}\ \xi_i^\mu\xi_j^\mu[(1+\varepsilon)\overline{S_j}-\varepsilon S_j]\right]. \tag{A2}$$

Proceeding as in Ref. [23], we obtain for the projections $m=(1/N)\Sigma_j\xi_j^1 S_j$ and $\overline{m}=(1/N)\Sigma_j\xi_j^1\overline{S_j}$ of the two-cycle on the retrieval pattern $\vec{\xi}^1$ at times t and $t+1$, respectively, and for the self-generated "noise" terms $r=(1/\alpha)\Sigma_{\mu\neq1}(m_\mu)^2$ and $\overline{r}=(1/\alpha)\Sigma_{\mu\neq1}[(1+\varepsilon)\overline{m}_\mu-\varepsilon m_\mu]^2$ in the zero temperature limit ($\beta\to\infty$) the coupled equations

$$\overline{m}=\mathrm{erf}(m/\sqrt{2\alpha r}), \tag{A3}$$

$$m=\mathrm{erf}\{[(1+\varepsilon)\overline{m}-\varepsilon m]/\sqrt{2\alpha\overline{r}}\}, \tag{A4}$$

$$r=\{[(1+\varepsilon)^2\overline{Q^2}+2(1+\varepsilon)\overline{Q\tilde{q}}]\}/N^2, \tag{A5}$$

$$\overline{r}=(\{(1+\varepsilon)^2+[(1+\varepsilon)\overline{Q}-\varepsilon]^2 +2(1+\varepsilon)[(1+\varepsilon)\overline{Q}-\varepsilon]q\})/N^2, \tag{A6}$$

$$N=1+\varepsilon\overline{Q}-(1+\varepsilon)Q\overline{Q}, \tag{A7}$$

$$Q=\sqrt{\frac{2}{\pi\alpha r}}\exp\left(-\frac{m^2}{2\alpha r}\right), \tag{A8}$$

$$\overline{Q}=\sqrt{\frac{2}{\pi\alpha\overline{r}}}\exp\left[-\frac{[(1+\varepsilon)\overline{m}-\varepsilon m]^2}{2\alpha r}\right], \tag{A9}$$

$$\tilde{q}=1-|m-\overline{m}|. \tag{A10}$$

For $|m-\overline{m}|\ll1$, i.e., $\tilde{q}\cong1$, Eqs. (A5) and (A6) for r and $\overline{r}$ can be solved in terms of Q and $\overline{Q}$ as

$$\sqrt{2\alpha r}=\sqrt{2\alpha}+\frac{2}{\sqrt{\pi}}\exp(-y^2), \tag{A11}$$

$$\sqrt{2\alpha\overline{r}}=\sqrt{2\alpha}+\frac{2}{\sqrt{\pi}}[(1+\varepsilon)\exp(-x^2)-\varepsilon\exp(-y^2)], \tag{A12}$$

where we introduced the reduced variables $x=m/\sqrt{2\alpha r}$ and $y=[(1+\varepsilon)\overline{m}-\varepsilon m]/\sqrt{2\alpha\overline{r}}$. With these, Eqs. (A2) and (A3) become

$$y\left[\sqrt{2\alpha}+\frac{2}{\sqrt{\pi}}[(1+\varepsilon)\exp(-x^2)-\varepsilon\exp(-y^2)]\right] =(1+\varepsilon)\mathrm{erf}(x)-\varepsilon\,\mathrm{erf}(y), \tag{A13}$$

$$x\left[\sqrt{2\alpha}+\frac{2}{\sqrt{\pi}}\exp(-y^2)\right]=\mathrm{erf}(y). \tag{A14}$$

By inserting x (as a function of y) from Eq. (A14) into Eq. (A13), we obtain a single equation for the variable y, which we write as

$$\frac{d}{dy}\Phi(y)=0. \tag{A15}$$

Since $y=\mathrm{erf}^{-1}(m)$, and the error function is monotonic (i.e., the relation between y and m is one to one), Eq. (A15) is equivalent to

$$\frac{d}{dm}L(m)=0, \tag{A16}$$

where $L(m)=\Phi[\mathrm{erf}^{-1}(m)]$ is the Lyapunov function of the Hopfield model. Thus $L(m)$ can be plotted as a function of m by integrating Eq. (A15), which yields $\Phi(y)$, and using $m=\mathrm{erf}(y)$. Figure 10 shows $L(m)$ as a function of α and ε.

[1] H. G. Schuster, *Deterministic Chaos* (VCH, Weinheim, 1994).
[2] E. Ott, C. Grebogi, and J. A. Yorke, Phys. Rev. Lett. **64**, 1196 (1990).
[3] T. Shinbrot, C. Grebogi, E. Ott, and J. D. Yorke, Nature (London) **363**, 411 (1993).
[4] E. R. Hunt, Phys. Rev. Lett. **67**, 1953 (1991).
[5] H. R. Roy, T. W. Murphy, T. D. Maier, A. Gill, and E. R. Hunt, Phys. Rev. Lett. **68**, 1259 (1992).
[6] H. G. Schuster, E. Niebur, E. R. Hunt, G. A. Johnson, and M. Löcher, Phys. Rev. Lett. **76**, 400 (1996).
[7] J. J. Hopfield, Proc. Natl. Acad. Sci. USA **79**, 2554 (1982); **81**, 3088 (1984).
[8] G. I. Sivashinsky and D. M. Michelson, Prog. Theor. Phys. **63**, 2112 (1980).
[9] K. Pyragas, Phys. Lett. A **170**, 421 (1992).
[10] S. Bielawski, M. Bouazaoui, D. Derozier, and P. Glorieux,

Phys. Rev. A **47**, R2492 (1993).
[11] M. Giona, Nonlinearity **4**, 911 (1991).
[12] More complicated periodic functions ε^t will also stabilize unstable orbits. The one chosen here is the simplest one.
[13] The d-dimensional map $\vec{x}^{t+1}=\vec{f}[\vec{x}^t+\varepsilon(t)(\vec{x}^t-\vec{x}^{t-1})]$ could be linearized around its fixed point $\vec{x}^*=0$ as $\vec{x}^{t+1}=M[\vec{x}^t+\varepsilon^t(\vec{x}^t-\vec{x}^{t-1})]$, where $M=(\partial f_i/\partial x_j)x^*$. By decomposing $\vec{x}^t$ into the right eigenvectors $\vec{e}_\lambda$ of M as $\vec{x}^t=\Sigma_\lambda \vec{e}_\lambda a_\lambda^t$, where λ are the eigenvalues of M, this becomes $a_\lambda^{t+1}=\lambda[(1+\varepsilon^t)a_\lambda^{t+1}-\varepsilon a_\lambda^t]$, i.e., a system of decoupled one-dimensional maps.
[14] L. Molgedey, J. Schuchhard, and H. G. Schuster, Phys. Rev. Lett. **69**, 3717 (1992).
[15] D. J. Amit, *Modelling Brain Function* (Cambridge University Press, Cambridge, 1989).
[16] D. J. Amit, *Modelling Brain Function* (Ref. [15]), p.190.
[17] M. Kerzberg and A. Zippelius, Phys. Scr. **33**, 54 (1990).
[18] G. M. Shepherd, *The Synaptic Organization of the Brain* (Oxford University Press, Oxford, 1990).
[19] R. Douglas, C. Koch, M. Mahowald, K. Martin, and H. Suarez, Science **269**, 981 (1995).
[20] The equation $\dot{x}=\lambda x(t)+\varepsilon^t[x(t)-x(t-\tau)]$ has the solution $x(t)=x(0)\exp(\lambda t)$ for $0\leqslant t<\tau$ and $x(t)=e^{(\lambda+\varepsilon)(t-\tau)}[x(\tau)-x(0)(1-e^{-\varepsilon(t-\tau)})]$ for $\tau\leqslant t<2\tau$ because we need to know $x^{t-\tau}$ only from the previous interval τ. This yields $x(2\tau)=e^{\lambda\tau}[(e^{\lambda\tau}-1)e^{\varepsilon\tau}+1]x(0)$. Since $(e^{\lambda\tau}-1)>0$ for $\lambda>0$, the factor $|e^{\lambda\tau}[(e^{\lambda\tau}-1)e^{\varepsilon\tau}+1]|$ remains larger than one for all values of ε, i.e., the fixed point cannot be stabilized.
[21] V. Petrov, E. Mihaliuk, S. K. Scott, and K. Showalter, Phys. Rev. E **51**, 3988 (1995).
[22] *Nonlinear Dynamics and Neuronal Networks*, edited by H. G. Schuster (VCH, Weinheim, 1991).
[23] J. Hertz, A. Krogh, and R. G. Palmer, *Introduction to the Theory of Neural Computation* (Addison-Wesley, New York, 1991), p. 36.